Economic Geology

BULLETIN OF THE SOCIETY OF ECONOMIC GEOLOGISTS

VOL. 107 March–April NO. 2

EXPRESS LETTER

A MAJOR LIGHT RARE-EARTH ELEMENT (LREE) RESOURCE IN THE KHANNESHIN CARBONATITE COMPLEX, SOUTHERN AFGHANISTAN

ROBERT D. TUCKER,[1,†] HARVEY E. BELKIN,[1] KLAUS J. SCHULZ,[1] STEPHEN G. PETERS,[1] FORREST HORTON,[2] KIM BUTTLEMAN,[1] AND EMILY R. SCOTT[3]

[1] *U.S. Geological Survey, National Center, MS 926A, 12201 Sunrise Valley Drive, Reston, Virginia 20192*

[2] *Department of Earth Science, University of California, Santa Barbara, California 93106-9630*

[3] *Task Force for Business Stability Operations, U.S. Department of Defense, 3600 Defense Pentagon, Washington, D.C. 20131*

Abstract

The rapid rise in world demand for the rare-earth elements (REEs) has expanded the search for new REE resources. We document two types of light rare-earth element (LREE)-enriched rocks in the Khanneshin carbonatite complex of southern Afghanistan: type 1 concordant seams of khanneshite-(Ce), synchysite-(Ce), and parisite-(Ce) within banded barite-strontianite alvikite, and type 2 igneous dikes of coarse-grained carbonatite, enriched in fluorine or phosphorus, containing idiomorphic crystals of khanneshite-(Ce) or carbocernaite. Type 1 mineralized barite-strontianite alvikite averages 22.25 wt % BaO, 4.27 wt % SrO, and 3.25 wt % $\sum LREE_2O_3$ (sum of La, Ce, Pr, and Nd oxides). Type 2 igneous dikes average 14.51 wt % BaO, 5.96 wt % SrO, and 3.77 wt % $\sum LREE_2O_3$. A magmatic origin is clearly indicated for the type 2 LREE-enriched dikes, and type 1 LREE mineralization probably formed in the presence of LREE-rich hydrothermal fluid. Both types of LREE mineralization may be penecontemporaneous, having formed in a carbonate-rich magma in the marginal zone of the central vent, highly charged with volatile constituents (i.e.,CO_2, F, P_2O_5), and strongly enriched in Ba, Sr, and the LREE. Based on several assumptions, and employing simple geometry for the zone of LREE enrichment, we estimate that at least 1.29 Mt (million metric tonnes) of $LREE_2O_3$ is present in this part of the Khanneshin carbonatite complex.

Introduction

Concern has risen about the future availability of rare-earth elements (REEs) because of China's dominance as the supplier of more than 97% of world REE output, their decision to restrict exports of rare-earth product, and the rapid increase in worldwide consumption of REE products (Long et al., 2010; Humphries, 2011; Kato et al., 2011; Roskill, 2011; U.S. Geological Survey, 2011). As a result, the United States, Japan, and member nations of the European Union may face a future of tight supplies and high prices unless other sources of REE are found and developed (Service, 2010). We report the mineralogy and petrology, and we estimate the grade and resource of a light rare-earth element (LREE) deposit in the Khanneshin carbonatite complex of southern Afghanistan. The deposit was previously delineated by Soviet scientists in the 1970s (Cheremitsyn and Yeremenko, 1976; Chmyrev, 1976; Vikhter et al., 1976; Alkhazov et al., 1978; Vikhter et al., 1978), and visited by us on three separate excursions, in 2009 to 2011, under the auspices of the U.S. Department of Defense and the Afghanistan Geological Survey (Peters et al., 2011; Tucker et al., 2011a, b).

The Khanneshin Carbonatite Complex

The Khanneshin carbonatite is a deeply dissected igneous complex of Pliocene-Quaternary age (Vikhter et al., 1978; Whitney, 2006) that rises 700 m above the Neogene sedimentary rocks of the Registan Desert, Helmand Province, Afghanistan. The complex consists almost exclusively of carbonate-rich intrusive and extrusive igneous rocks, crudely circular in outline, with three small hypabyssal plugs of foid silicate that crop out in the southeastern part of the complex (Fig. 1). The igneous complex is broadly divisible into a central intrusive vent, approx. 4 km in diameter, consisting of coarse-grained sövite and dike-intruded agglomeratic alvikite,

† Corresponding author: e-mail, rtucker@usgs.gov

*A digital supplement to this paper is available at <http://economicgeology.org/>

©2012 by *Economic Geology*, Vol. 107, pp. 197–208
0361-0128/12/4008/197-12

Submitted: November 3, 2011
Accepted: December 23, 2012

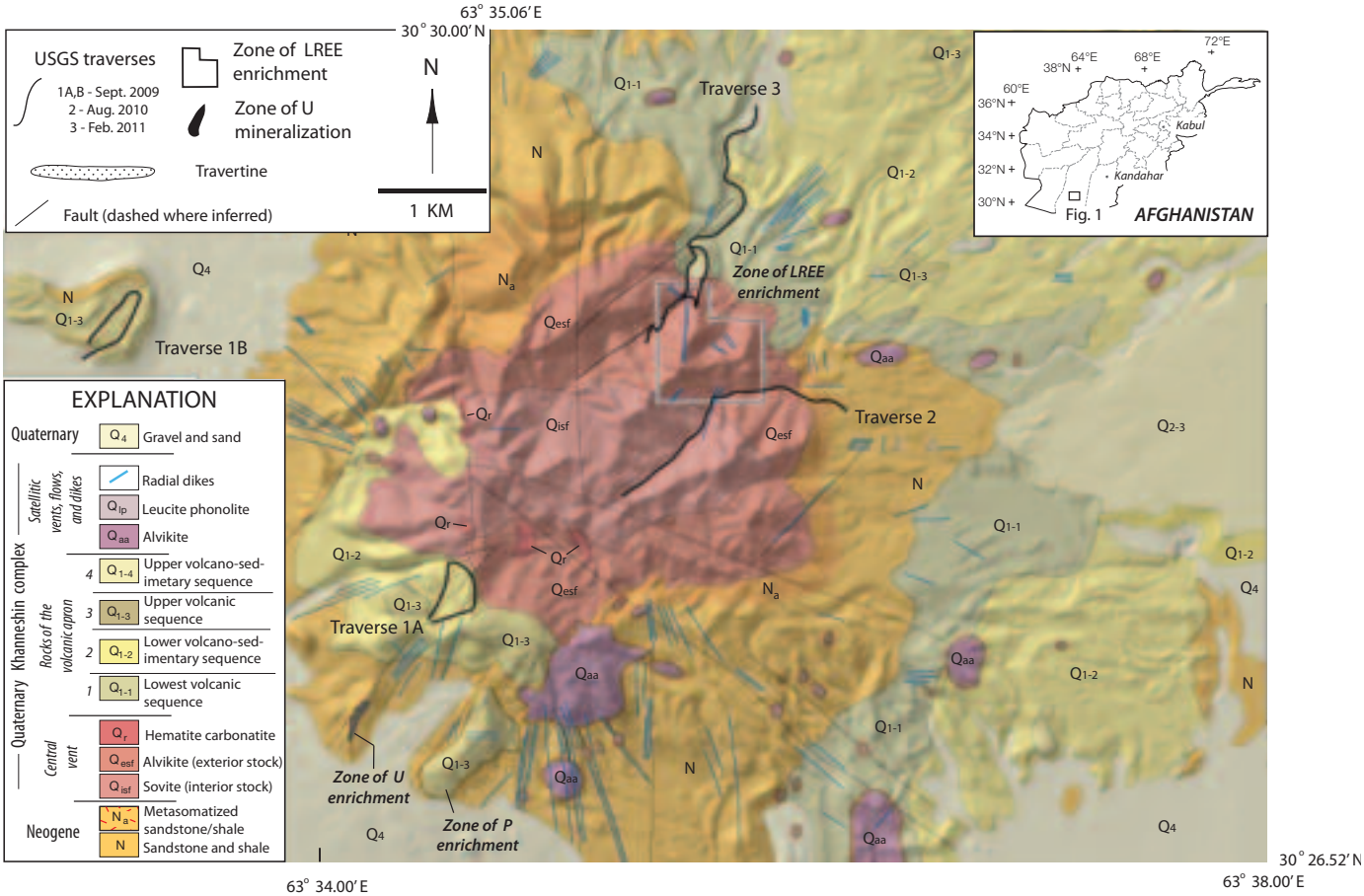

FIG. 1. Geologic map of the Khanneshin carbonatite complex showing its principal bedrock divisions (bottom to top in Explanation): (1) Neogene sedimentary strata, partly metasomatized, that form an upturned section of outwardly-dipping strata away from the central intrusive vent. (2) The central intrusive vent composed of sövite, medium- to fine-grained alvikite, and altered hematite-stained carbonatite. The zone of LREE enrichment is located in the northeast portion of the central vent. (3) The apron of volcanic and volcanosedimentary strata extending 5 km beyond from the central vent. (4) Small satellitic intrusions and volcanic plugs, mostly on the southern peripheral margin of the complex, of alvikite agglomerate and leucite phonolite. Our traverses, 1A, 1B, 2, and 3, as well as the zones of LREE, uranium, and phosphorus enrichment, are indicated by labels.

a thin marginal zone (<1 km wide) of outwardly dipping (5°–45°) and alkali-metasomatized Neogene sedimentary strata, and a peripheral apron of volcanic and volcaniclastic strata extending another 3 to 5 km away from the central intrusive vent (Fig. A1; Tucker et al. 2011a, b). Small satellitic intrusions, no larger than 400 m in diameter, of agglomeratic alvikite, sövite, and rare leucite phonolite crop out on the southern and southeastern margin of the central intrusive vent.

Ore mineralogy

In the 1970s, Soviet geologists (Cheremitsyn and Yeremenko, 1976; Chmyrev, 1976) identified an area approx. 0.64 km² in the outer, northeast portion of the central intrusive vent, underlain by alvikite highly enriched in barium, strontium, and the LREE (Fig. 1). In two exploratory visits to the area, we identified two types of LREE mineralization throughout all of that area indicated as the "zone of LREE enrichment" in Figure 1. Type 1 LREE mineralization consists of layered barite-strontianite alvikite with discontinuous seams of LREE carbonate minerals that are oriented parallel (concordant) with the bulk-rock layering (Fig. 2A). The type 1 seams are 0.5 to 0.7 m thick and several tens of meters long, and they are commonly banded symmetrically with a light-colored outer margin about a dark central zone (Fig. 2A, B). The minerals in the light-colored margin consist of khanneshite-(Ce), barite, strontianite, and secondary synchysite-(Ce) and parisite-(Ce). The dark central zone, consisting primarily of ankeritic dolomite, barite, apatite, and strontianite, also has trace khanneshite-(Ce). In some seams, the LREE carbonates form dense spherical-shaped aggregrates (100 µm diam), interpreted as immiscible droplets, that make up as much as 30% (by volume) of the seam (Fig. 2D, E). In other seams, the LREE-rich margins display a breccia texture (Fig. 2C), indicating that a hydrothermal fluid, or fluid-rich magma, rich in LREE, Ba, and Sr, penetrated the barite-strontianite alvikite at a late stage. These type 1 seams alternate with meter-thick layers of barite-strontianite alvikite (wall rock) over a vertical thickness of approximately 150 m. The estimated ratio of wall rock to mineralized seams throughout the section of barite-strontianite alvikite is approximately 10:1.

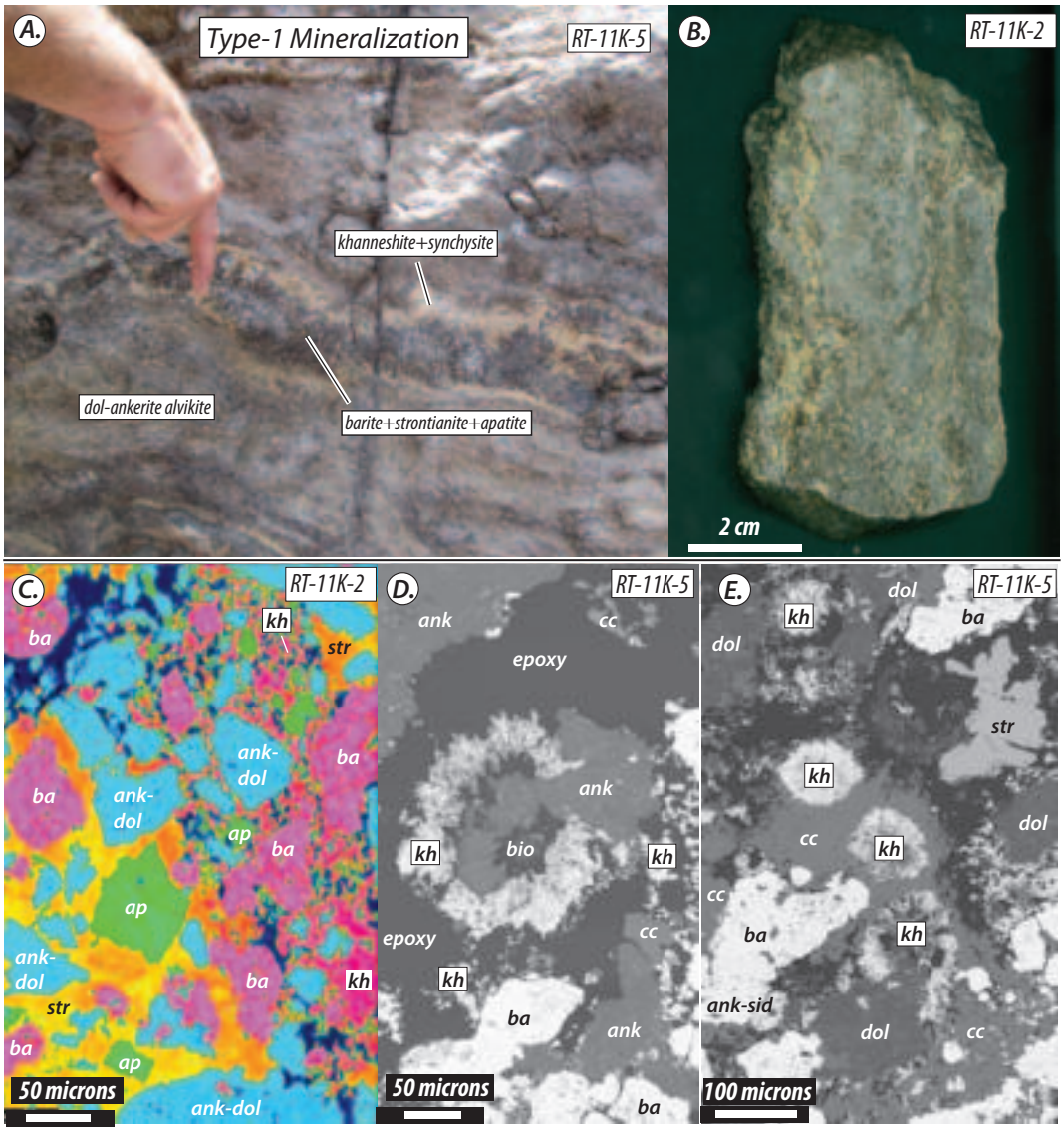

FIG. 2. Type 1 concordantly mineralized rocks and textures. (A) Banded dolomite-ankerite alvikite and the type 1 concordant mineralized seams at station RT-11K-5. The symmetrically banded seams of mineralized alvikite consist of two outer margins, enriched in khanneshite-(Ce) and synchysite-(Ce), and a dark central zone of barite-strontianite-apatite alvikite. These mineral seams alternate, on the scale of centimeters, with typical barite-strontianite alvikite over a vertical thickness of approximately 150 m. The mineral seams are grossly parallel, or concordant, with the layering in the barite-strontianite alvikite and hence they define the type 1 style of mineralization. (B) Slab of the symmetrically zoned type 1 alvikite, showing the light-colored khanneshite-(Ce) and synchysite-(Ce)-rich bands, and the dark-colored barite-strontianite-apatite-rich central zone. (C) False-colored backscattered electron image of the brecciated margin of a khanneshite-(Ce) and synchysite-(Ce)-rich band. (D) and (E) The interior zone of barite-strontianite-apatite alvikite. The interior zones also have LREE-carbonate minerals including spherical domains (immiscible droplets?) of khanneshite-(Ce) and synchysite-Ce) within interstitial calcite and ankerite. Early-formed minerals include dolomite, ankerite, barite, and strontianite. Mineral abbreviations: ank = ankerite, ank-dol = ankeritic-dolomite, ank-sid = ankerite-siderite, ba = barite, bio - biotite, cc = calcite, kh = khanneshite-(Ce), str = strontianite.

Type 2 LREE mineralization occurs in igneous dikes composed of euhedral to subhedral crystals that precipitated directly from carbonatite magma or a late-stage hydrothermal fluid. Type 2 igneous dikes, which intrude the type 1 mineralized alvikites, are of two types (Fig. 3): those enriched in fluorine and those enriched in phosphorus. The fluorine-rich dikes contain euhedral to subhedral crystals (or fine aggregates) of khanneshite-(Ce), monazite-(Ce), and fluorite, together with synchysite-(Ce), bastnäsite-(Ce), and calkinsite-(Ce) of likely secondary (late hydrothermal) origin (Fig. 3E, F); taeniolite ($KLiMg_2Si_4O_{10}F_2$) is present as a rare accessory mineral. Of the type 2 dikes rich in fluorine, the general sequence of LREE-Sr-Ba mineralization: Sr-LREE-Ca-Na rich carbonates (khanneshite-(Ce)) → Ca-REE fluorocarbonates (bastnäsite-(Ce)) → Ca-LREE hydrated carbonate (calkinsite-(Ce)) (Tucker et al., 2011a). The phosphorus-rich igneous dikes contain subhedral crystals of carbocernaite, and interstitial apatite, together with parisite-(Ce) of secondary origin (Fig.

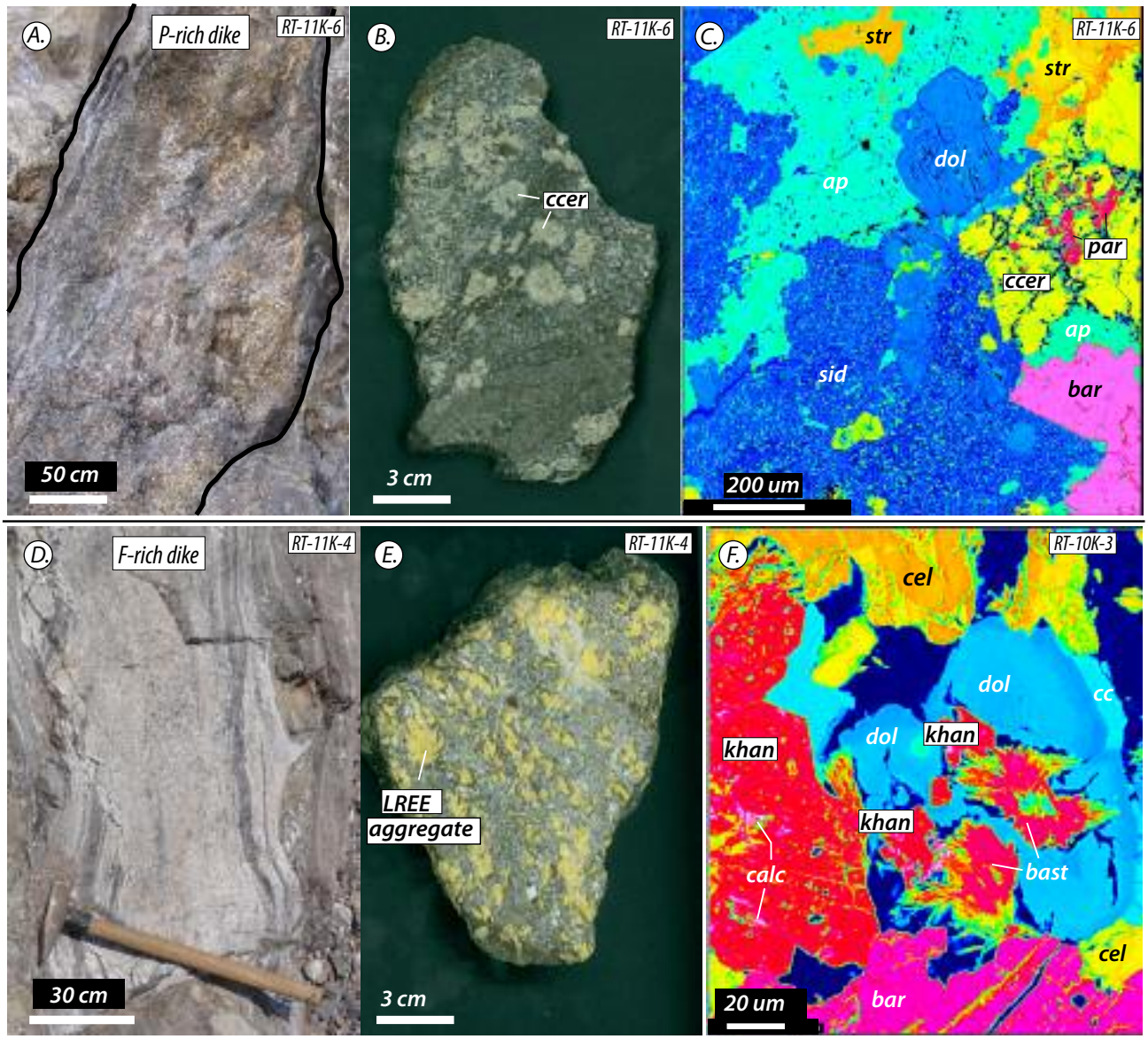

FIG. 3. Examples of type 2 mineralized igneous dikes in the zone of LREE-enrichment. Type 2 phosphorus-rich dikes (A-C). Type 2 fluorine-rich dikes (D-F). (A) Apatite-bearing carbonatite dike, with local pegmatitic texture, at field station RT-11K-6. The carbonatite dike, approximately 75 cm thick and steeply dipping, intrudes the concordantly banded type 1 mineralized alvikite (top left). (B) Apatite-bearing carbonatite dike, RT-11K-6, showing the large subhedral crystals of carbocernaite (ccer) in a matrix of dolomitic-ankerite, apatite, barite, and strontianite. (C) False-colored backscattered electron image showing the textural relationships among carbocernaite (ccer), dolomite-ankerite (dol), siderite (sid), barite (bar), strontianite (str), and apatite (ap). Dolomitic ankerite, with siderite rims, and carbocernaite form early phenocrysts; apatite, strontianite, and barite form interstitial minerals; and parisite-(Ce) (par) forms a late alteration mineral of carbocernaite (ccer). (D) Fluorine-rich carbonatite dike (RT-11K-4) that intrudes the banded alvikites of the marginal zone, intrusive central vent. (E) Fluorine-rich carbonatite dike, RT-11K-4, showing the large subhedral aggregates of yellow LREE-carbonates in a fine-grained matrix of dolomite, barite, strontianite, and calcite. (F) False-colored, backscattered electron image of a fluorine-rich dike (RT-10K-3): bastnäsite-(Ce) (bast), barite (bar), calcite (cc), calkinsite-(Ce) (calc), celestine (cel), dolomite (dol), khanneshite-(Ce) (khan), Khanneshite-(Ce) are idiomorphic crystals, surrounded by interstitial dolomite and calcite. Bastnäsite-(Ce) and calkinsite-(Ce) are late alteration minerals of khanneshite-(Ce), dolomite, and calcite.

3B, C). Of the type 2 dikes rich in phosphorus, a general sequence of LREE-Sr-Ba mineralization is Sr-LREE-Ca-rich carbonate (carbocernaite) → Ca-LREE fluorocarbonate (parisite-(Ce) → Sr-LREE hydrated carbonate (ancylite-(Ce). Most type 2 igneous dikes are 50 to 60 cm thick and traceable for tens of meters; at least three of the type 2 dikes, particularly those rich in fluorine, are 10 to 50 m thick and traceable for hundreds of meters (Chmyrev, 1976).

Ore geochemistry and grade

There is compelling evidence for multiple generations and distinctive types of carbonatite magma. Soviet geologists

identified two sequences of volcanic strata (Fig. 1, $Q_{1\text{-}1}$ and $Q_{1\text{-}3}$) in the peripheral apron that are separated by a sequence of volcanosedimentary rocks ($Q_{1\text{-}2}$) (Cheremitsyn and Yeremenko, 1976). These stratified rocks are intruded by several small hypabyssal intrusions (Q_{aa}) and numerous carbonatite dikes with crude radial geometry. Most importantly, in the critical zone of LREE enrichment, ankerite alvikite and carbonatite dikes of the central vent were fully crystalline before the mineralized barite-strontianite alvikites, rich in LREE, were emplaced above them (Fig. A1B) (Tucker et al., 2011a). These LREE-enriched alvikites are intruded by fluorine- and phosphorus-rich carbonatite dikes which may be the plumbing for the upper alvikite section. These dikes are also highly enriched in Ba, Sr, and LREE (i.e., type 2 mineralization).

The banded barite-strontianite alvikites are chemically distinctive (Fig. 4, Fig. A2, Tables A1–A3):

1. They contain as much as ~4 wt % MnO (Table A3, Fig. A2A) and they have major and accessory amounts of manganoan ankerite, ferroan rhodochrosite, pyrolusite, and manganosite.
2. As their mineralogy implies, they are highly enriched in strontium and barium (Fig. 4A, B). In typical alvikite and sövite of the volcanic apron and central vent (Tables A1, A2), strontium and barium average 10,000 and 3,000 ppm, respectively. In the zone of LREE-enrichment (Table 1), barite-strontianite alvikite averages 22.25 wt % BaO and 4.27 wt % SrO. In rare instances, BaO and SrO exceed 30 and 8 wt %, respectively (Table 1, A3).
3. They are also enriched in fluorine and sulfur as indicated by the ubiquitous presence of fluorite, F-bearing minerals (i.e., synchysite, parasite, bastnäsite, and taeniolite), barite, and less commonly, celestine.

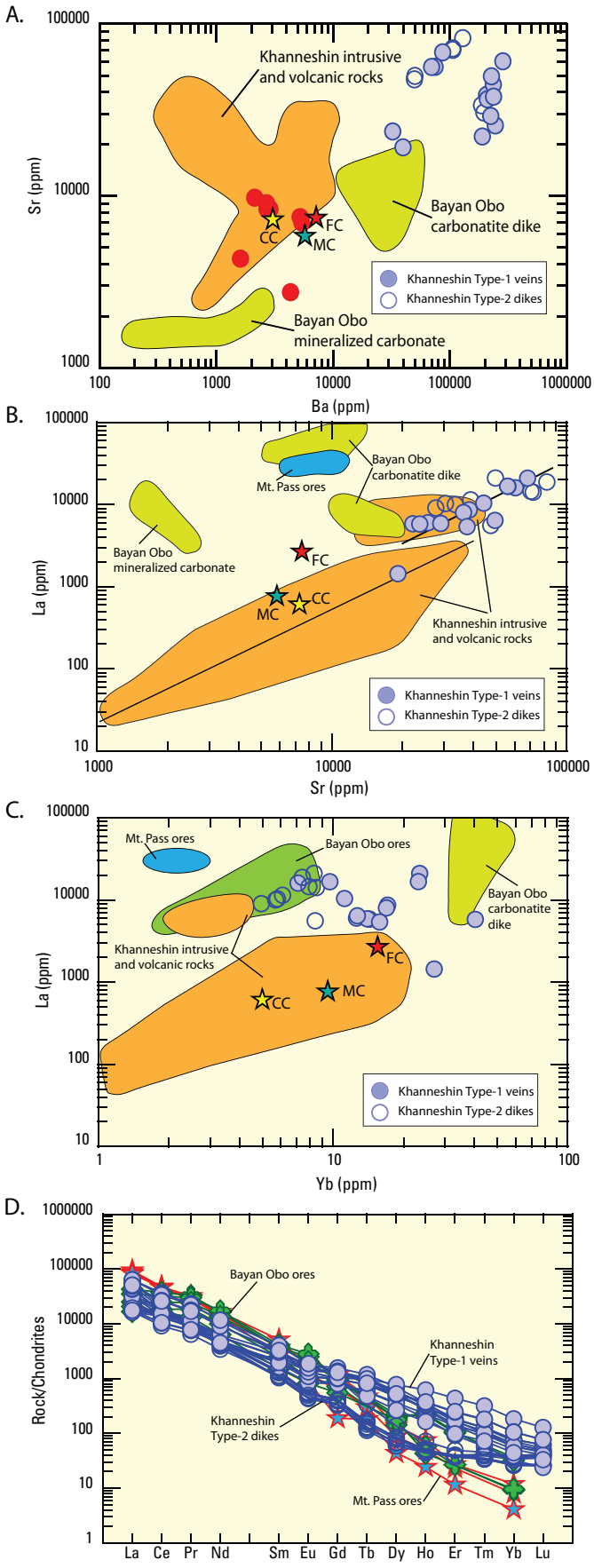

FIG. 4. Diagrams illustrating the magnitude and significance of LREE enrichment in the marginal zone, central intrusive vent, Khanneshin carbonatite complex. Red circles are volcanic tuffs and dikes from the southwest part of the Khanneshin complex (Table A1). Blue circles, filled and unfilled, are LREE-enriched rocks from the LREE zone (Table A3). The shaded orange area is the field for Khanneshin intrusive and volcanic rocks sampled in 2009 and 2010 (Table A2). Average calciocarbonatite (CC, yellow star), ferrocarbonatite (FC, red star), and magnesiocarbonatite (MC, black star) data are from Woolley and Kempe (1989). Also shown are the minimum, mean, and maximum grades of the REE ores from Mountain Pass (Castor, 2008) and Bayan Obo (Yuan et al., 1992; Yang et al., 2009). (A) Sr (ppm) versus Ba (ppm). Note the high concentrations of Ba and Sr, in the LREE-enriched rocks of the Khanneshin complex relative to average calcio-, ferro-, and magnesio-carbonatites, the Bayan Obo carbonatite dike, and common alvikites, sövites, and dikes of the Khanneshin carbonatite complex (Tables A1-A3). (B) La (ppm) versus Sr (ppm). The positive correlation of the LREE and Sr in the REE-enriched rocks indicates the propensity of the LREE to substitute for Sr in khanneshite (burbankite group) and carbocernaite, the primary carbonate minerals of the Khanneshin complex. Also shown are mineralized carbonate and carbonatite dikes from Byan Obo and average ores from Mountain Pass, California. (C) La (ppm), representative of the LREE, versus Yb (ppm) representative of the HREE. Common alvikites of the Khanneshin complex have LREE and HREE concentrations similar to average ferro-, magnesio-, and calcio-carbonatites world-wide. However, the ankerite-barite alvikites of the marginal central vent, Khanneshin complex, are highly enriched in the REE and comparable in grade to the world-class REE deposits of Bayan Obo and Mountain Pass. (D) Whole-rock concentration data, traverse 3 samples, normalized relative to chondrite values. Same symbols as B, above.

TABLE 1. Summary of BaO, SrO, and Light Rare-Earth Element ($LREE_2O_3$) Concentrations, in the Zone of LREE Enrichment, Khanneshin Carbonatite Complex, Afghanistan

Sample no.	Deposit type[1]	BaO (wt %)	SrO (wt %)	La_2O_3 (wt %)	Ce_2O_3 (wt %)	Pr_2O_3 (wt %)	Nd_2O_3 (wt %)	Sm_2O_3 (wt %)	Eu_2O_3 (wt %)	Gd_2O_3 (wt %)	Tb_2O_3 (wt %)	Dy_2O_3 (wt %)	Ho_2O_3 (wt %)	Er_2O_3 (wt %)	Tm_2O_3 (wt %)	Yb_2O_3 (wt %)	Lu_2O_3 (wt %)	$\sum LREE_2O_3$[2] (wt %)
RT-11K-1A1	2-F	21.92	3.60	1.208	1.710	0.130	0.336	0.0299	0.0046	0.0126	0.0008	0.0030	0.0004	0.0010	0.0001	0.0007	0.0001	3.38
RT-11K-1A2	2-F	24.03	4.62	1.337	1.850	0.139	0.354	0.0310	0.0048	0.0133	0.0009	0.0033	0.0004	0.0010	0.0001	0.0007	0.0001	3.68
RT-11K-1B2	2-F	20.93	3.97	1.173	1.721	0.136	0.356	0.0322	0.0050	0.0126	0.0009	0.0033	0.0004	0.0010	0.0001	0.0006	0.0001	3.39
RT-11K-2A2	1	21.27	2.62	0.680	1.040	0.098	0.319	0.0452	0.0086	0.0257	0.0032	0.0142	0.0018	0.0035	0.0003	0.0016	0.0002	2.14
RT-11K-2B1	1	23.12	4.55	1.009	1.370	0.118	0.360	0.0481	0.0099	0.0312	0.0042	0.0186	0.0024	0.0046	0.0004	0.0019	0.0002	2.86
RT-11K-2B2	1	23.47	4.30	0.927	1.312	0.116	0.357	0.0484	0.0098	0.0308	0.0042	0.0184	0.0024	0.0046	0.0004	0.0019	0.0002	2.71
RT-11K-3B31	2-P	26.39	5.24	1.220	1.429	0.111	0.316	0.0516	0.0124	0.0423	0.0055	0.0208	0.0021	0.0035	0.0003	0.0013	0.0002	3.08
RT-11K-3B32	2-P	31.91	7.15	1.877	1.944	0.138	0.354	0.0380	0.0075	0.0255	0.0031	0.0135	0.0015	0.0024	0.0002	0.0008	0.0001	4.31
RT-11K-4AO1	2-F	5.57	5.62	0.645	0.930	0.084	0.252	0.0268	0.0044	0.0106	0.0007	0.0026	0.0004	0.0010	0.0001	0.0010	0.0002	1.91
RT-11K-4AO2	2-F	14.43	9.75	2.205	2.061	0.137	0.323	0.0252	0.0040	0.0125	0.0007	0.0027	0.0004	0.0010	0.0001	0.0008	0.0001	4.73
RT-11K-4B3	2-F	11.87	8.33	1.701	1.698	0.119	0.296	0.0251	0.0040	0.0110	0.0007	0.0027	0.0004	0.0010	0.0001	0.0009	0.0001	3.81
RT-11K-4C1A	2-F	11.85	8.51	1.654	1.628	0.116	0.288	0.0244	0.0038	0.0104	0.0006	0.0023	0.0004	0.0010	0.0001	0.0010	0.0002	3.69
RT-11K-4C1B	2-F	4.44	2.26	0.169	0.276	0.029	0.098	0.0219	0.0056	0.0191	0.0028	0.0138	0.0021	0.0051	0.0006	0.0031	0.0004	0.57
RT-11K-5A2	1	27.47	3.03	0.703	1.522	0.145	0.430	0.0588	0.0127	0.0402	0.0051	0.0208	0.0023	0.0038	0.0003	0.0014	0.0002	2.80
RT-11K-5A3	1	25.07	3.44	0.689	1.452	0.139	0.417	0.0594	0.0130	0.0425	0.0055	0.0231	0.0026	0.0042	0.0004	0.0016	0.0002	2.70
RT-11K-5B1B	1	26.51	4.46	0.631	1.393	0.138	0.420	0.0589	0.0126	0.0406	0.0053	0.0231	0.0027	0.0048	0.0004	0.0018	0.0002	2.58
RT-11K-5B3B	1	25.46	5.86	0.751	1.557	0.149	0.465	0.0726	0.0157	0.0497	0.0064	0.0271	0.0029	0.0044	0.0003	0.0014	0.0002	2.92
RT-11K-5B6A	1	5.62	5.89	2.463	3.689	0.304	0.827	0.0762	0.0118	0.0316	0.0018	0.0053	0.0006	0.0013	0.0002	0.0009	0.0002	7.28
RT-11K-6A2A	2-P	3.62	2.80	0.679	1.057	0.102	0.328	0.0461	0.0097	0.0322	0.0053	0.0305	0.0050	0.0112	0.0011	0.0046	0.0005	2.17
RT-11K-6A2B	2-P	9.72	8.07	2.452	3.408	0.290	0.851	0.0947	0.0162	0.0434	0.0043	0.0201	0.0030	0.0063	0.0006	0.0027	0.0003	7.00
RT-11K-6B2	2-P	8.37	6.65	1.947	2.693	0.232	0.676	0.0713	0.0118	0.0322	0.0026	0.0104	0.0013	0.0025	0.0002	0.0011	0.0001	5.55
RT-11K-6B3	2-P	7.82	6.64	1.959	2.623	0.221	0.662	0.0766	0.0139	0.0413	0.0044	0.0207	0.0030	0.0064	0.0006	0.0026	0.0003	5.47

	(wt %)	(wt %)	Summary table	(wt %)	(wt %)	(wt %)	(wt %)	(wt %)
	Δ BaO	Δ SrO		Δ La_2O_3	Δ Ce_2O_3	Δ Pr_2O_3	Δ Nd_2O_3	Δ $LREE_2O_3$
	22.25	4.27	Type 1 mineralized barite-strontianite alvikite (samples RT-11K-2, -5)	0.98	1.67	0.15	0.45	3.25
	14.64	6.09	Type 2 phosphorus-rich dikes (samples RT-11K-3, -6)	1.69	2.19	0.18	0.53	4.59
	14.38	5.83	Type 2 fluorine-rich dikes (samples RT-11K-1, -4)	1.26	1.48	0.11	0.29	3.14
	14.51	5.96	All type 2 dikes (samples RT-11K-1, -3, -4 and -6)	1.44	1.79	0.14	0.39	3.77
	17.31	5.33	Type 1 and 2 LREE-enriched rocks	1.28	1.74	0.15	0.41	3.58

[1] Type 1 barite-strontianite alvikite, 2-F = type 2 fluorine-rich dike, 2-P = type 2 phosphorus-rich dike

[2] $\sum LREE_2O_3$ is the sum of La_2O_3, Ce_2O_3, Pr_2O_3, and Nd_2O_3 rounded to three significant figures; Δ is the average value of the oxide element

4. Most importantly, they are highly enriched in the REE and, in common with carbonatites worldwide (Woolley and Kempe, 1989), they are strongly enriched the LREE over the HREE (Fig. 4D).

The type 2 mineralized igneous dikes have $LREE_2O_3$ grades that compare favorably with the world's largest producers of REE: Bayan Obo, China (Yuan et al., 1992; Yang et al., 2009), and Mountain Pass, California (USA) (Castor, 2008). Our type 2 dikes range in grade between 0.57 and 7.00 wt % ($LREE_2O_3$) and they average 3.77 wt % ($LREE_2O_3$, Table 1). There is only a slight difference in grade among our samples (standard deviation = 1.62) and no discernible difference between the average type 1 ores and type 2 igneous dikes. Type 1 ores, for example, have an average LEE_2O_3 grade of 3.25 wt % (range, 2.14–7.28 wt %, std. dev. = 1.65, n = 8), whereas the phosphorus-rich type 2 dikes have a slightly higher average LEE_2O_3 grade of 4.59 wt % (2.17– 7.00 wt %, std. dev. = 1.98, n = 6). Although the concentrations of LREE greatly exceed the heavy REE (HREE), both type 1 and 2 rocks are enriched in HREE relative to the ores of Bayan Obo and Mountain Pass (Fig. 4C, D).

Within the total population of barite-strontianite alvikites, there is a positive correlation between the concentration of phosphorus and the HREE, suggesting that apatite rather than REE-carbonate is the principal carrier of the HREE in the type 1 barite-strontianite alvikites. Type 1 alvikites contain abundant apatite and up to 40 ppm Yb, a proxy for the HREE (Fig. A2D), whereas type 2 igneous dikes are relatively poor in apatite (with 0.1–0.3 wt % P_2O_5) and contain less than 10 ppm Yb.

LREE Resource Estimation

Estimated tonnage of type 1 ore

Based on Soviet work (Cheremitsyn and Yeremenko, 1976; Chmyrev, 1976) that accurately describes the geology and mineralogy of the igneous complex, we assume the type 1 alvikites are present throughout the area of LREE enrichment. This assumption is justified by the many samples of "REE ore" recovered and analyzed by Soviet geologists, and by our mineralogical descriptions and whole-rock chemical analyses that confirm their observations. The volume of LREE mineralization of type 1, however, must be diluted by a factor of 10, which is approximately the ratio of common barite-strontianite alvikite (wall rock) to the concordant seams enriched in khanneshite-(Ce) and synchysite-(Ce) (Fig. 2A). This dilution factor is a conservative value because, in some sections, concordant mineralization is ubiquitous, whereas in other sections, the surface exposures are sparse or covered by alluvium.

Exploratory drilling, core analysis, and airborne geophysical surveys are not currently possible, so the depth of mineralization is estimated from ground observations. We assert a value of 150 m based on the thickness of LREE-enriched barite-strontianite alvikite observed over the rugged relief of the region (~170 m). In essence, we assume a depth of mineralization that roughly mimics the young surface topography. This assumption is justified because the intrusive massif is less than 600 ka (Whitney, 2006), the valley walls are steep and, hence, the mass of eroded rock is small relative to the unexhumed mass at depth. We believe, moreover, our estimate is conservative if, as seems likely, the zone of LREE enrichment extends to depths well beyond the arbitrary value of 150 m. Using an average density of mineralized carbonatite (2.94 g/cc), an average grade of LREE concentration (3.25 wt %, Table 1), and a dilution factor of 10:1 (wall rock: LREE seams), we calculate approximately 0.71 Mt of $LREE_2O_3$ are present in the type 1 ores throughout the zone of LREE enrichment (Table 2).

Estimated tonnage of type 2 ore

A second type of LREE mineralization occurs in igneous dikes of carbonatite that intrude and are feeders of the LREE-rich barite-strontianite alvikites. The carbonatite dikes are enriched in fluorine and/or phosphorus and contain well-formed crystals of khanneshite-(Ce) and carbocernaite, respectively. Within the zone of LREE enrichment, more than 50 such "orebodies" of a "stockwork-type," with widths between 60 m and 500 cm and lengths between 500 and 20 m, are identified by Cheremitsyn and Yeremenko (1976) and Chmyrev (1976). These correspond to the igneous dikes illustrated in Figure 3. The depth of the dikes is likely to be hundreds of meters because they form near-vertical sheets that transect the rugged relief of the region and their source was a magma chamber at depth. Thus, we assume a minimum depth of 150 m and a uniform grade of $LREE_2O_3$ throughout their length and breadth. A dilution factor is not applied to the type 2 igneous dikes because they consist uniformly of coarse- and medium-grained igneous minerals, multiple samples yield consistent LREE concentrations, and the dikes display little evidence of extensive wall rock assimilation.

We estimate a tonnage of $LREE_2O_3$ for just three of the largest dikes within the zone of LREE enrichment (Table 2). Assuming average carbonatite density (2.94 g/cc) and grade of $LREE_2O_3$ concentration (3.77 wt %, Table 1), we estimate an $LREE_2O_3$ resource of 0.58 Mt in three type 2 dikes (Table 2). This figure is approximately 45% of the total resource, the sum of type 1 and 2 ores, within the zone of LREE enrichment (i.e., 1.29 Mt, Table 2). The estimated total resource (1.29 Mt) is almost an order of magnitude greater than the current, annual tonnage (134,000 t) of $LREE_2O_3$ consumed worldwide (Humphries, 2011). Moreover, it is consistent with our estimation of $LREE_2O_3$ resources (1.37 Mt, Table 2), calculated in an area with similar spectral characteristics in the marginal central vent that overlaps and extends beyond the Soviet-defined zone (Tucker et al., 2011a). Both estimates comport well with the probabilistic estimate of 1.4 Mt of undiscovered REE resources in all of south Afghanistan (Peters et al., 2007).

Because of current security and logistical concerns in this part of Afghanistan, our resource estimate is preliminary and probably conservative. Clearly, more ground and aerial surveys, together with remote-sensing studies, must be completed when local conditions allow. Despite this, the estimated LREE resource at Khanneshin represents a significant fraction of global REE resources or about half of available reserves at Mountain Pass, California (5% grade cutoff), and about 2.5% (perhaps less) of reserves at Bayan Obo, China (Haxel et al., 2002; Long et al., 2010). Quite clearly, the

TABLE 2. Estimated Tonnage of Type 1 and 2 $LREE_2O_3$ Resources, Khanneshin Carbonatite Complex, Afghanistan

	Length (km)	Width (km)	Depth (km)	Volume (km^3)	Density (g/cm^3)	Rock mass (10^6 Mt)	Δ $LREE_2O_3$ grade (wt %)[1]	Mt $LREE_2O_3$ (before 10:1 dilution)[2]	Mt $LREE_2O_3$ (after dilution)
Zone of LREE enrichment (Fig. 1)									
Type 1. Concordant veins and seams									
Northern zone	0.750	0.550	0.150	0.0619	2.94	181.91	3.25	5.91	0.59
Southern zone	0.330	0.250	0.150	0.0124	2.94	36.38	3.25	1.18	0.12
Type-1 total				0.0743	2.94	218.30	3.25	7.09	0.71
Type 2. Discordant igneous dikes[3]									
no. 1	0.050	0.020	0.150	0.0002	2.94	0.44	3.77		0.02
no. 2	0.500	0.040	0.150	0.0030	2.94	8.82	3.77		0.33
no. 3	0.400	0.035	0.150	0.0021	2.94	6.17	3.77		0.23
Type-2 total				0.0053	2.94	15.44	3.77		0.58
Total LREE enrichment [4]									1.29
Remote sensing polygon (Tucker et al., 2011a, Fig. 1)									
NW of zone of LREE enrichment				0.071	2.94	209.26	3.25	6.80	0.68
Within zone of LREE enrichment				0.073	2.94	214.98	3.25	6.98	0.70
Total remote sensing polygon									1.38

[1] Average $LREE_2O_3$ grade for type 1 and 2 rocks from Table 1
[2] Wall rock is 10 times more abundant than mineralized seams, hence 10:1 dilution factor
[3] Includes both fluorine- and phosphorus-rich dikes
[4] Sum of Type 1 and 2 tonnage

LREE at Khanneshin represents a very valuable and strategic resource within Afghanistan's substantial inventory of mineral commodities. Our new LREE assessment is part of a larger report, released this year for the Department of Defense Task Force for Business Stability and Operations (TFBSO) which also includes a revised evaluation of their principal deposits of gold, silver, iron, copper, lead, zinc, phosphorus, and uranium (Peters et al., 2011).

Acknowledgments

This research was funded by the Task Force for Business and Stability Operations, U.S. Department of Defense, as a contract agreement with the U.S. Geological Survey. Transportation, accommodation, and security during field work to the Khanneshin carbonatite complex were provided by the U.S. Department of Defense. We thank Associate Editor Watanabe for his thorough and constructive review of our manuscript.

REFERENCES

Alkhazov, V. Yu, Atakishiyev, Z.M., and Azimi, N.A., 1978, Geology and mineral resources of the early Quaternary Khanneshin carbonatite volcano (southern Afghanistan), International Geology Review, v. 20, p. 281–285.

Castor, S.B., 2008, The Mountain Pass rare-earth carbonatite and associated ultrapotassic rocks, California, The Canadian Mineralogist, v. 46, p. 779–806.

Cheremitsyn, V.G., and Yeremenko, G.K., 1976, Report of the Hanneshin crew on the results of prospecting and evaluational activity for 1976, Kabul, Afghanistan: Afghanistan Geological Survey Report 1142, 84 p., 7 maps, scale 1:10,000. (in Russian)

Chmyrev, V.M., 1976, Report of the Nuristan crew on the results of geological prospecting for solid commercial mineral deposits in Afghanistan, 1975, Kabul, Afghanistan: Afghanistan Geological Survey Report 1028, Section B, no. 5, p. 92–103. (in Russian)

Haxel, G.B., Hedrick, J.B., and Orris, G.J., 2002, Rare-earth elements—critical resources for high technology: U.S. Geological Survey Fact Sheet 087-02, 4 p.

Humphries, M., 2011, Rare-earth elements: The global supply chain: Library of Congress, Congressional Research Service (CRS) Report for Congress, R41347, 26 p.

Kato, Y., Funjinaga, K., Nakamura, K., Takaya, Y., Kitamura, K., Ohta, J., Toda, R., Nakashima, T., and Iwamori, H., 2011, Deep-sea mud in the pacific ocean as a potential resource for rare-earth elements: Nature doi: 10.1038/NGEO1185.

Long, K.R., Van Gosen, B.S., Foley, N.K., and Cordier, Daniel, 2010, The principal rare-earth elements deposits of the United States—A summary of domestic deposits and a global perspective: U.S. Geological Survey Scientific Investigations Report 2010-5220, 96 p. (http://pubs.usgs.gov/sir/2010/5220/.

Peters, S.G., Ludington, S.D., Orris, G.J., Sutphin, D.M., and Bliss, J.D., eds., 2007, Preliminary non-fuel mineral resource assessment of Afghanistan: U.S. Geological Survey Open-File Report 2007-1214, 810 p.

Peters, S.G., King, T.V.V., Mack, T.J., Chornack, eds., and the U.S. Geological Survey Afghanistan Mineral Assessment Team, 2011, Summaries of important areas for mineral investment and production opportunities of nonfuel minerals in Afghanistan: U.S. Geological Survey Open-File Report V. II, 2011-1204, 1,810 p. plus appendixes on DVD (http://pubs.usgs.gov/of/2011/1204/).

Roskill, 2011, Rare-earths & yttrium: Market outlook to 2015 [14th edition]: Information Services Ltd., 492 p.

Service, R.F., 2010, Nations move to head off shortages of rare-earths: Science, v. 327, p. 1596–1597.

Tucker, R.D., Belkin, H.E., Schulz, K.J., Peters, S.G., and Buttleman, K.P., 2011a, Rare-earth element mineralogy, geochemistry, and preliminary resource assessment of the Khanneshin carbonatite complex, Helmand Province, Afghanistan: U.S. Geological Survey Open-File Report 2011-1207, 50 p. (http://pubs.usgs.gov/of/2011/1207/).

Tucker, R.D., Peters, S.G., Schulz, K.J., Renaud, K.M., Stettner, W.R., Masonic, L.M., and Packard, P.H., compilers, 2011b, Geologic map of the Khanneshin carbonatite complex, Helmand province, Afghanistan [modified from the 1976 original map compilation of V.G. Cheremytsin]: U.S. Geological Survey Open-File Report 2011–1244, one sheet, scale 1:10,000. (http://pubs.usgs.gov/of/2011/1244/).

U.S. Geological Survey, 2011, Mineral commodity summaries 2011: U.S. Government Printing Office, 198 p.

Vikhter, B. Ya., Yeremenko, G.K., and Chmyrev, V.M., 1976, A young volcanogenic carbonatite complex in Afghanistan: International Geology Review, v. 18, p. 1305–1312.

Vikhter, B. Ya., Yeremenko, G.K., Chmyrev, V.M., and Abdulla, D., 1978, Pliocene-Quaternary volcanism of Afghanistan, International Geology Review, v. 20, p. 525–536.

Whitney, J.W., 2006, Geology, water, and wind in the lower Helmand Basin, southern Afghanistan: U.S. Geological Survey Scientific Investigations Report 2006-5182, 40 p.

Woolley, A.R., and Kempe, D.R.C., 1989, Carbonatities: Nomenclature, average chemical compositions, and element distributions, *in* Bell, Keith, ed., Carbonatites—genesis and evolution: London. Unwin Hyman, p. 1–14.

Yang, X-Y., Sun, W-D., Zhang, Y-X., and Zheng, Y-F., 2009, Geochemical constraints on the genesis of the Bayan Obo Fe-Nb-REE deposit in Inner Mongolia, China: Geochimica et Cosmochimica Acta, v. 73, p. 1417–1435.

Yuan, Z., Bai, G., Wu, C., Zhang, Z., and Ye, X., 1992, Geological features and genesis of the Bayan Obo REE ore deposit, Inner Mongolia, China: Applied Geochemistry, v. 7, p. 429–442.

Appendix: Supporting Supplementary Material

Analytical Methods

Bulk-rock analyses: Major element contents of bulk-rock samples from the Khanneshin carbonatite complex were measured at laboratories of the U.S. Geological Survey (Denver, Colorado) and ActLabs (Ontario, Canada) by wavelength dispersive X-ray fluorescence spectrometry and ICP-MS, respectively. Details of the analytical procedures at the USGS laboratory are given in Briggs and Meier (2002) and Taggart and Seims (2002), and those of ActLabs may be found at http://www.actlabs.com/page.

Trace element and REE abundances our bulk rock samples were made in three laboratories. Trace element and REE abundances of traverse 1 samples, from the southwestern part of the carbonatite complex, were determined by ICP-MS at the USGS analytical laboratory (Denver, Colorado) using a Perkin Elmer Elan 6000 mass spectrometer after bulk rock powder decomposition in a mixture of hydrochloric, nitric, perchloric, and hydrofluoric acids (Briggs and Meier, 2002). The REE abundances of traverse 1 samples were replicated by the ICP-MS method after sintering of bulk rock powders

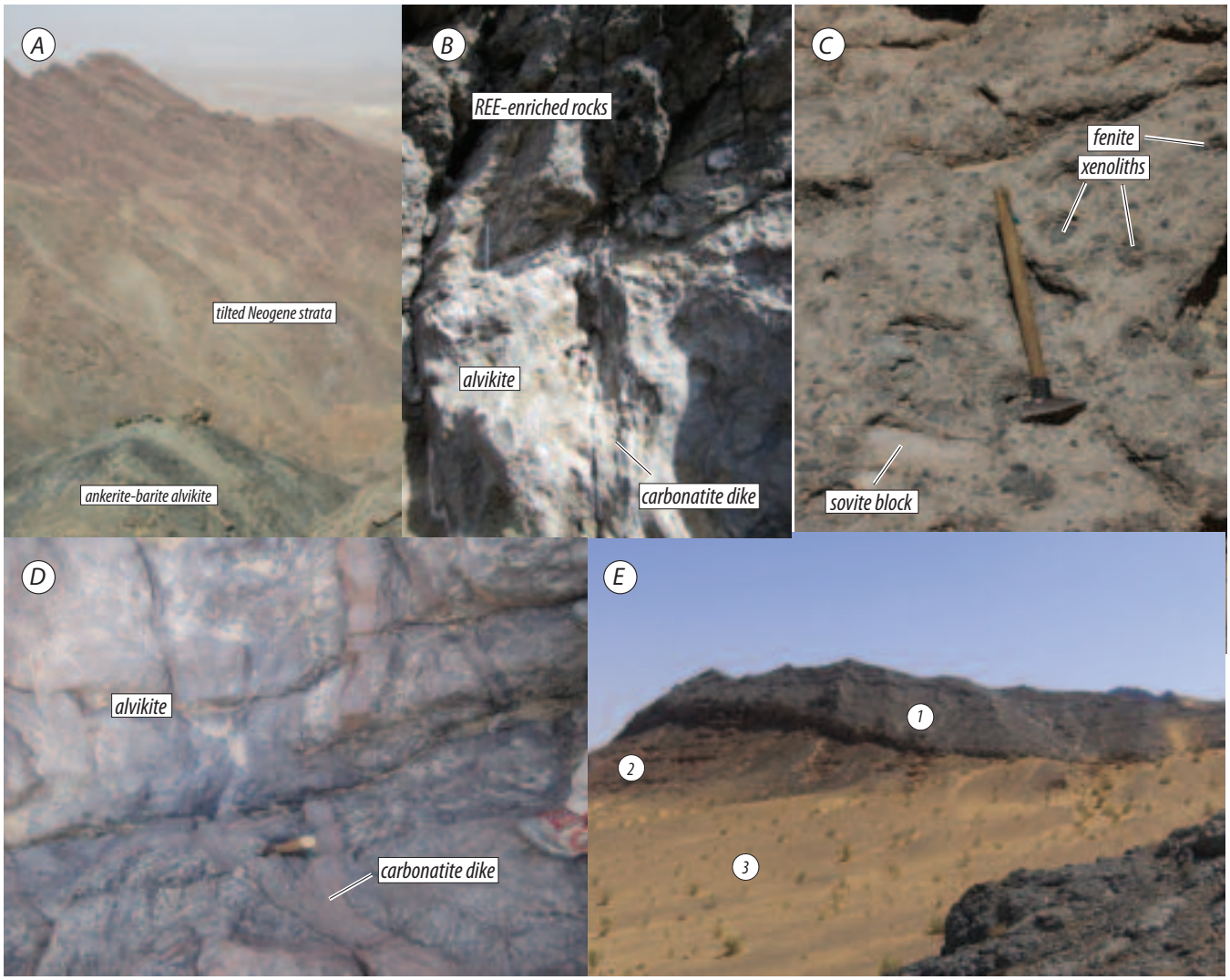

FIG. A1. Field photographs showing the key rock types and relationships within the intrusive central vent and volcanic apron of the Khanneshin carbonatite complex, Afghanistan. (A) Northwest view from the zone of rare-earth element (REE) enrichment showing the Neogene strata (background) dipping modestly north and away from the intrusive rocks of the central vent (foreground). Vertical relief is approximately 150 m (note person in the foreground for scale). (B) Unconformable relationship between LREE-enriched barite-strontianite alvikite (above) and typical alvikite of the marginal zone, intrusive central vent. The underlying alvikite was solid and intruded by a carbonatite dike before emplacement of the overlying LREE-enriched alvikite. (C) Common fine-grained alvikite in the marginal zone of the central vent contains abundant xenoliths of fenitized country rock ("glimmerite") and sövite. (D) Alvikite of the central vent, here also with xenoliths, is intruded by fine-grained dikes of carbonatite. (E) View of the volcanic rocks (1 in circle) of the western apron ($Q_{1\text{-}3b}$) showing their relationship to older Neogene strata (2 in circle, N) and younger Quaternary gravels (3 in circle, Q_4).

with sodium peroxide, leaching with water, and dissolution in nitric acid to assure complete digestion of the REE. Trace element and REE abundances of traverse 2 samples, from the southern part of the LREE zone, were determined at Stewart Assay and Environmental Laboratories (LLC) by ICP-MS following total fusion with a sodium peroxide flux. Trace element and REE abundances of traverse 3 samples, our most enriched samples from the northern part of the LREE zone, were determined by ICP and ICP-MS, in ActLabs commercial laboratory, following bulk-rock fusion with a lithium metaborate/tetraborate flux. These bulk rock samples were prepared as per code 4B of ActLabs laboratory (http://www.actlabs.com), spiked with internal standards to cover the entire mass range from vanadium to uranium, and analyzed by Perkin Elmer SCIEX ELAN 6100 and 9000 ICP-MS. All analyses are generally within 2% of accepted values of standard reference materials issued by the U.S. Geological Survey and reproducibility of replicate analyses (n = 5) is typically <3% RSD.

Mineral identification: Mineral identification was achieved by optical petrography, energy-dispersive spectroscopy (EDS)

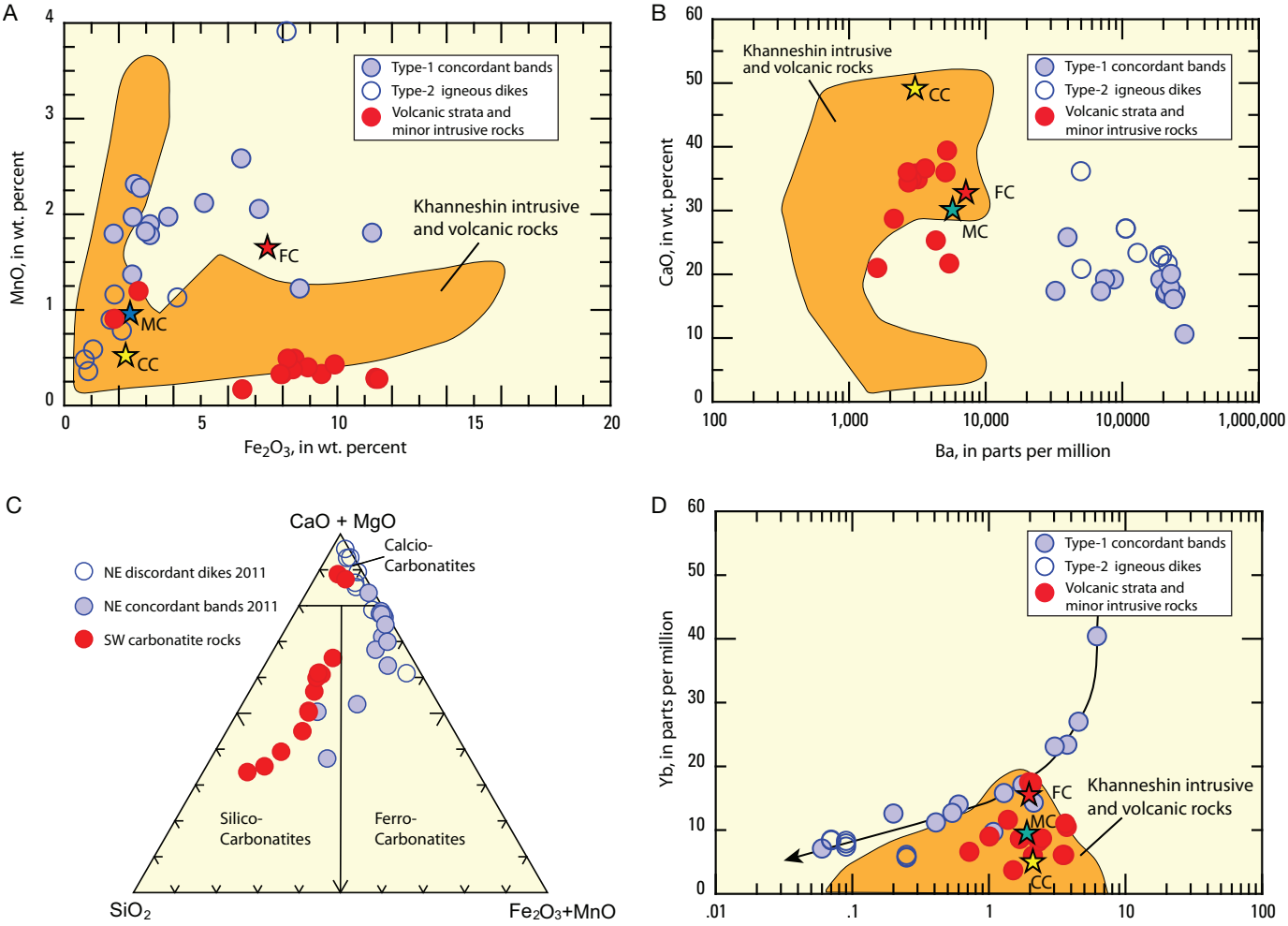

FIG. A2. (A-D) Variation diagrams illustrating the major- and trace-element characteristics among igneous rocks of the Khanneshin carbonatite complex, Afghanistan (symbols as in Fig. 4). The orange field delineates the common intrusive and extrusive igneous rocks from traverses 1 and 2 (Tables A1, A2). Average values of calicocarbonatite (yellow star), ferrocarbonatite (red star), and magnesiocarbonatite (blue star). Blue circles, filled and unfilled, represent the mineralized rocks within the zone of LREE enrichment of the northeast margin of the central intrusive vent. (A) MnO versus Fe_2O_3 (wt %). Note the enrichment of MnO in the type 1 mineralized rocks over common alvikite of the Khanneshin complex. (B) CaO (wt %) versus Ba (ppm) (1% (parts per hundred) = 10,000 ppm). Note the very high concentrations of Ba in LREE-enriched rocks of the Khanneshin carbonatite complex. (C) Ternary diagram of the major elements, illustrating the difference between bulk rocks from the northeast and southwest parts of the complex. Red circles are volcanic strata and minor intrusive rocks from the southwest part of the complex (Fig. 1, traverses 1A, B). Filled blue circles are type 1 mineralized rocks; open blue circles are type 2 mineralized dikes. Type 1 and 2 mineralized rocks from the zone of LREE enrichment are noticeably depleted in silica, relative to the volcanic rocks and dikes from southwest part of the complex. (D) Yb (ppm) versus log P_2O_5 (wt %). The type 1 mineralized rocks and type 2 intrusive dikes having modal apatite and carbocernaite are enriched in Yb and the heavy rare-earth elements (HREE). The positive correlation between Yb and P_2O_5, particularly the type 1 ores, suggests that apatite hosts most of the HREE. Most of the LREE are hosted within LREE carbonate minerals (i.e., khanneshite-(Ce), synchysite-(Ce), bastnäsite-(Ce)). The fluorine-rich type 2 dikes, bearing either fluorite or an unidentified K-Mg-F phase, are poor in apatite and HREE.

and backscattered electron imaging using a JEOL JXA-8900R scanning electron microprobe equipped with an EDS analysis system. The Si(Li) crystal EDS Noran Instrument detector had a nominal resolution of 138 eV. For additional confirmation for elements such as F and Ce, we used qualitative wavelength dispersive X-ray spectrometry; the LDE1 analyzing crystal was used for the F K line, and the LIF analyzing crystal was used for the Ce Lβ1 line. Appropriate wavelength dispersive X-ray spectrometers were peaked-up on standards of known composition at the National Center of the U.S. Geological Survey, Reston, Virginia.

APPENDIX REFERENCES

Briggs, P.H. and Meier, A.L., 2002, The determination of forty-two elements in geological materials by inductively coupled plasma-mass spectrometry, *in* Taggart, J.E., Jr., ed., Analytical methods for chemical analysis of geologic and other materials, U.S. Geological Survey Open-File Report 02-223, I1-I14.

Taggart, J.E., Jr. and Siems, D.F., 2002, Major element analysis by wavelength dispersive X-ray fluorescence spectrometry, *in* Taggart, J.E., Jr., ed., Analytical methods for chemical analysis of geologic and other materials: U.S. Geological Survey Open File Report 02-223, T1-T9.